LASER-BASED BEAM DIAGNOSTICS*

G. A. Blair, Royal Holloway Univ. of London, Egham, Surrey TW20 0EX,UK.

Abstract

Lasers are increasingly being employed in particle beam diagnostics. Laser-based techniques are attractive because they are essentially non-invasive to the beam under test and can not be destroyed by it. They also have the potential to be extremely fast. Uses include transverse beam profile measurement at electron machines using the Compton effect and at proton machines using laser-ionization of H- beams. An introduction is provided to Gaussian beam propagation and how this affects the laser properties and final focus optics needed for the various applications. Recent applications and results from ongoing research projects will be reviewed, with particular emphasis on the "laser-wire" systems recently employed at the PETRA and ATF machines. Future possibilities will be discussed, including higher order laser modes and interferometric techniques.

INTRODUCTION

Future electron machines will need accurate determination and monitoring of their transverse phase space in order to meet their challenging performance specifications. A detailed analysis of the issues and challenges involved in such measurements are presented in Ref. [1], with particular reference to the International Linear Collider (ILC) [2]; a brief summary of this work is presented below in order to motivate the challenges of the laser and optics prestented later.

The Laser-Wire (LW) is a key beam diagnostics, which is useful for beam profiles ranging from several tens of microns, down to the micron scale. Smaller beam profiles have been measured using laser interferometric techniques [3, 4] whereas traditional solid wires or screens can be used for larger profiles (although they are disruptive to the electron beams). Very challenging, low f-number, laser optics are necessary for the LW in order to achieve the required small laser spot-sizes and the subsequent performance is evaluated numerically and described in below. The laser systems necessary to power the LW are also very challenging and the necessary specifications are next derived and discussed.

TRANSVERSE EMITTANCE MEASUREMENT

The International Linear Collider (ILC) has demanding emittance goals that will need to be measured accurately in order to maximise the machine performance; the parameters of the ILC [2] are presented in Tab. 1, which provides the context for the requirements on measurement beam spot sizes and scanning speeds, discussed below.

Table 1: Nominal ILC Parameters

Beam energy	E	250(500) GeV
Norm. horiz. emittance	$\gamma\epsilon_x$	10^{-5}m rad
Norm. vert. emittance	$\gamma\epsilon_y$	$4 \cdot 10^{-8}$ m rad
Train repetition rate	f	5 Hz
Num. bunches per train	$N_{\rm train}$	2625
Inter-bunch spacing (ns)		369
Bunch length	L_b	300 μm
Num. electrons per bunch	N_e	2×10^{10}

Beam Phase Space

The phase-space of a general Gaussian particle beam can be described by four-dimensional (4d) matrix:

$$\sigma = \begin{bmatrix} \langle x^2 \rangle & \langle xx' \rangle & \langle xy \rangle & \langle xy' \rangle \\ \langle xx' \rangle & \langle x'^2 \rangle & \langle x'y \rangle & \langle x'y' \rangle \\ \langle xy \rangle & \langle x'y \rangle & \langle y^2 \rangle & \langle yy' \rangle \\ \langle xy' \rangle & \langle x'y' \rangle & \langle yy' \rangle & \langle y'^2 \rangle \end{bmatrix} \quad (1)$$

The standard approach to reconstructing the 4d coupled beam matrix with the least-squares fit method is presented in Ref [5]. At a scanner location in the beam-line it is possible to measure three values, $\langle x^2 \rangle$, $\langle y^2 \rangle$ and $\langle xy \rangle$, with the help of a horizontal (x), a vertical (y), and a tilted (u) wire scanner, as illustrated in Fig. 1, where the tilt-scanning angle, ϕ, is also defined.

The optimal value for ϕ is given by

$$\phi_0 = \tan^{-1}\left(\frac{\sigma_x}{\sigma_y}\right) . \quad (2)$$

and typical values of interest to the ILC beam delivery system (BDS) are presented in Tab. 2.

The ten independent entries of Eq. 1 can be obtained either by changing the optics in a controlled manner at the wire location [6, 5, 7] or by locating the wires at different positions in the beam-line. The latter technique will be relevant for routine fast-scanning operation at the ILC. Here it will be assumed that six laser-wire scanning stations are located at optimal locations in the BDS and that each laser-wire station measures x,y and u with the same relative measurement error. The emittance can then be inferred by inverting the relations between the transverse spot

* Work supported by the UK Science and Technology Facilities Council and by the Commission of European Communities under the 6th Framework Programme Structuring the European Research Area, contract number RIDS-01189.

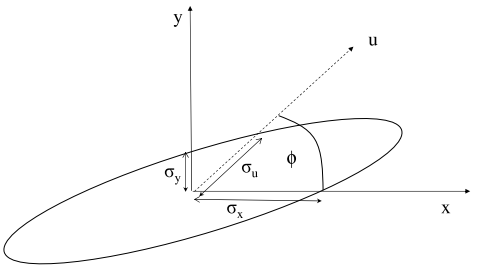

Figure 1: *Bunch with horizontal-vertical coupling, such that its major axis does not lie along the horizontal. In addition to vertical and horizontal scans, a scan of the u-axis is necessary, where u is at an angle ϕ to the vertical as shown.*

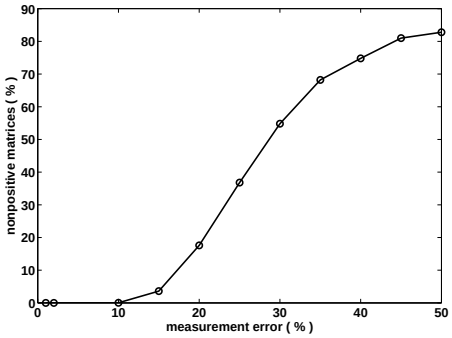

Figure 2: *Beam matrix rejection fraction vs. relative beam size measurement error level for the 4d ILC emittance measurement section with 6 scanners [1].*

Table 2: *The relevant measurables for emittance measurement under the approximation $\langle xy \rangle \simeq 0$ for a set of electron beam sizes of interest at the ILC for the given beam energies E_b.*

E_b GeV	σ_x μm	σ_y μm	ϕ_0 deg	σ_u μm	σ_v μm
500	9	1.4	81.2	1.95	8.89
500	15	1.4	84.7	1.97	14.9
250	14	2	81.8	2.8	13.8
250	20	1.8	84.8	2.53	19.9

sizes as given by the R-matrices relating the beam twiss parameters at each location. This may lead to an unphysical result (a non-positive beam matrix) when the measurement is sufficiently noisy. A typical dependency of the fraction of non-positive matrices on the relative measurement error is shown in Fig. 2, where it can be seen that the relative error should be kept below about 10% if significant reconstruction inefficiency is to be avoided.

The quality of emittance reconstruction by performing this technique is shown in Fig 3, which motivates the need for LW systems that can measure beam spotsizes to a few percent (or better). Methods for achieving such accuracies will now be discussed.

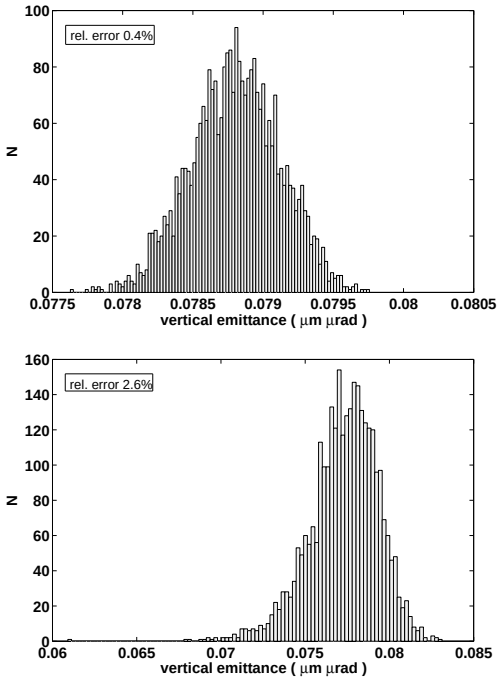

Figure 3: *Distribution of reconstructed vertical emittance with 1% (a) and 5% (b) random errors on the beam size measurement for a 4d diagnostics section (statistics corresponding to train length). Initial optical functions are perfectly matched. The true emittance is 0.079 $\mu m \cdot \mu rad$ [1].*

GAUSSIAN BEAM OPTICS

Paraxial Approximation

Maxwell's equations in free space lead to electromagnetic field solutions of the form $E(x, y, z) \exp(ickt)$

where:

$$\left(\frac{\partial^2}{\partial x^2}+\frac{\partial^2}{\partial y^2}+\frac{\partial^2}{\partial z^2}+k^2\right)E(x,y,z)=0 \qquad (3)$$

A pure plane wave travelling in the x-direction has the exact solution $E(x,y,z) = E_0\exp(ikx)$ but, due to diffraction effects, this is not in general sufficient to describe a laser beam of finite transverse size. Assuming a solution of the form $E(x,y,z) = u(x,y,z)\exp(-ikx)$ in Eq. 3 gives:

$$\left(\frac{\partial^2}{\partial z^2}+\frac{\partial^2}{\partial y^2}+\frac{\partial^2}{\partial x^2}-2ik\frac{\partial}{\partial x}\right)u(x,y,z)=0 \qquad (4)$$

In most practical situations, any variations along the beam (i.e. along x) will be gradual, which enables the $\partial^2u/\partial x^2$ term to be ignored. As explained in Ref. [12], this so-called paraxial approximation is valid provided any rays within the beam are traveling at angles less than about 0.5 radians with respect to the optical axis, which is true for all the practical cases described later. The paraxial wave equation is then:

$$\frac{\partial u(x,y,z)}{\partial x}=-\frac{i}{2k}\left(\frac{\partial^2}{\partial z^2}+\frac{\partial^2}{\partial y^2}\right)u(x,y,z) \qquad (5)$$

The TM_{00} Mode

Consider a Gaussian beam with an intensity (which is proportional to the square of the field strength) profile of the form:

$$I(x,y,z)=|u(x,y,z)|^2=\frac{I_0}{2\pi\sigma^2(x)}\exp\left(-\frac{y^2+z^2}{2\sigma^2(x)}\right) \qquad (6)$$

where I_0 is the (constant) total power of the beam and the first factor of $\sigma(x)^{-2}$ is the normalisation necessary to keep the total power constant as a function of x. For the simplest laser mode (TM_{00}) there is no azimuthal dependence and so the problem can be formulated using $r=\sqrt{y^2+z^2}$ and solving:

$$2ik\frac{\partial u}{\partial x}=\frac{\partial^2u}{\partial r^2}+\frac{1}{r}\frac{\partial u}{\partial r} \qquad (7)$$

in the form

$$u(x,r)=\sqrt{\frac{I_0}{2\pi}}\frac{1}{\sigma(x)}\exp\left(-\frac{r^2}{4\sigma^2(x)}\right)e^{i\phi(x,r)} \qquad (8)$$

Substituting Eq. 8 into Eq. 7, and solving, yields:

$$\sigma(x)=\sigma_0\left[1+\left(\frac{x}{x_R}\right)^2\right]^{\frac{1}{2}} \qquad (9)$$

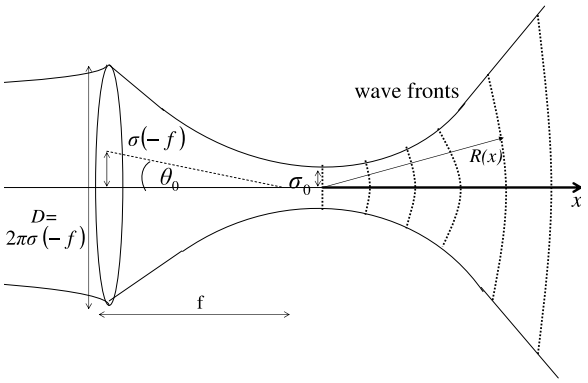

Figure 4: *The key features of the focussing of a Gaussian beam through a circular aperture of diameter D and focul length f. The beam has its waist at a distance $\simeq f$ from the lens, at which point its intensity distribution has Gaussian rms σ_0; this point also defines $x = 0$. The curvature of the wavefronts $R(x)$ varies as fuction of distance x from the waist, and is infinite at $x = 0$ and $x = \infty$. At large distances from its waist the beam diverges linearly with distance $\sigma = x\tan\theta_0$, where $\tan\theta_0 = \sigma(-f)/f$.*

where x_R, the so-called Rayleigh range, is given by

$$x_R=\frac{4\pi\sigma_0^2}{\lambda}, \qquad (10)$$

λ is the laser wavelength and

$$\phi(x,r)=\tan^{-1}\left(\frac{x}{x_R}\right)-\frac{2\pi}{\lambda}r^2\frac{\sigma'(x)}{\sigma(x)}. \qquad (11)$$

The first term of Eq. 11 shows that there is a phase shift of π (the Guoy phase shift) on passing through the focus, defined as where $\sigma(x)$ is a minimum; this point also defines $x = 0$. The second term of Eq. 11 is intepreted as due to the curvature of the wavefront, which can be written in terms of a radius of curvature $R(x)$ given by:

$$R(x)=x+\frac{x_R^2}{x}. \qquad (12)$$

This interpretation of the solution in terms of Gaussian-spherical waves is illustrated in Fig. 4; a more general treatment of this interpretation is given in Ref. [12].

When x is large compared to x_R, the beam diverges linearly:

$$\sigma(-f)\simeq\frac{\sigma_0}{x_R}f=\frac{\lambda f}{4\pi\sigma_0} \qquad (13)$$

and

$$\theta_0=\tan^{-1}\left(\frac{\sigma(-f)}{f}\right)\simeq\frac{\lambda}{4\pi\sigma_0} \qquad (14)$$

The usual practical convention [12] is to require 99% of energy in the Gaussian beam profile to be contained within

the lens aperture, here assumed to be circular with diameter D. For the TM_{00} mode this requirement means:

$$0.99 = \int_0^{D/2} \int_0^{2\pi} r dr d\phi \frac{1}{2\pi\sigma(-f)^2} \exp\left[-\frac{r^2}{2\sigma(-f)^2}\right] \quad (15)$$

so $D \simeq 2 \times \pi\sigma(-f)$ and by substituting this into Eq. 13

$$D \simeq 2\pi \frac{\lambda f}{4\pi\sigma_0} \quad (16)$$

$$\sigma_0 = 0.5\lambda f_{\#} \, . \quad (17)$$

where the f-number is defined by $f_{\#} = f/D$. In this case, the opening angle $\theta = 1/f_{\#}$ between the centre of the diverging Gaussian beam and its e^{-2} intensity cone is given by:

$$\theta = \frac{\lambda}{\pi\sigma} = \frac{1}{f_{\#}}$$

and so, for TM_{00} with f_1 optics, $\sigma_0 = \lambda/\pi$ and $\theta = 1$ rad, or 57°. Thus, for $f_{\#} > 1$, the maximum angle of divergence of any ray in the beam is of order 0.5 rad, so the paraxial approximation is valid.

In practice, the laser beam must be transported over large distances involving many optical components and significant alignment challenges; so the practical final aperture D may be smaller than the nominal aperture of the final focus lens. For this reason it is safer to assume a more conservative final practical beam spot size $\sigma_\ell = k_p\sigma_0$ where k_p includes all the practical aspects of laser transport and alignment. In Ref. [1], and in the following analysis, $k_p \simeq 2$ is taken as a conservative estimate. So from now on the laser rms intensity at the waist, σ_ℓ, is given by the conservative estimate:

$$\sigma_\ell \simeq \lambda f_{\#} \quad (18)$$

The literature of laser optics contains several definitions of "laser spot size". It is common to find the beam size defined in terms of the diameter of the beam, where the radius of the beam is defined by the point $x = w$ at which the beam intensity is $1/e^2$ of its maximium value. In the above notation, this occurs at $x = 2\sigma$. To compare notation, $w = 2\sigma$ and the "laser spot size" is then $2w$, or 4σ. In the following, everything will be evaluated using σ but care is needed when comparing with formulae in other references.

Higher Order Laser Transverse Modes

In practice, the laser will not produce a pure TM_{00} mode but will also include higher order transverse modes. To illustrate the impact of such modes on the beam propagation issues, consider the TM_{01} mode where the condition that 99% of the light energy is contained within the lens aperture becomes:

$$0.99 = \int_0^{D_\ell/2} \int_0^{2\pi} r dr d\phi \frac{1}{2\pi\sigma_\ell^2} \left(\frac{r}{\sigma_\ell}\right)^2 \sin^2\phi \exp\left[-\frac{r^2}{2\sigma_\ell^2}\right] \quad (19)$$

which gives

$$0.01 = \left(1 + \frac{D_\ell^2}{8\sigma_\ell^2}\right) \exp\left[-\frac{D_\ell^2}{8\sigma_\ell^2}\right] \quad (20)$$

and hence $D_\ell \simeq 1.15 \times 2\pi\sigma_\ell$. So this means that the effective size of the beam is increased if TM_{01} modes are present. The same will be true for even higher order modes and their combined effect is included in a practical M^2 value for the laser, where $M^2 \geq 1$, with $M^2 = 1$ corresponding to a perfect laser.

The formulae outlined above for Gaussian laser optics are very similar to those used in accelerator physics, which describe a charged particle beam using a β-function and and emittance ϵ. The β-function is defined by the machine optical systems, such that the beam profile at any point is given by

$$\sigma_x = \sqrt{\epsilon\beta} \quad (21)$$

$$\sigma_{x'} = \sqrt{\epsilon/\beta} \quad (22)$$

$$\sigma_x\sigma_{x'} = \epsilon \quad (23)$$

where $\sigma_{x'}$ is the rms of the angular distribution. So, while the local profile of the beam depends on the β-function, the product $\sigma_x\sigma_{x'}$ at any location is invariant.

Comparing this with the formulae derived above for a perfect TM_{00} Gaussian laser beam; using Eq. 14 the corrsponding invariant is given by

$$\sigma_x\sigma_{x'} = \sigma_0\theta_0 = \frac{\lambda}{4\pi} \quad (24)$$

The effects of higher-order transverse modes are then taken into account by increasing the "emittance" of the laser beam to:

$$\sigma_x\sigma_{x'} = M^2\frac{\lambda}{4\pi} \quad (25)$$

If no re-tuning of the optical system is performed, then the effect of increasing M^2 is to increase both the local spot size and the angular divergence by a factor M, as shown in Fig. 5.

However, in practice, the laser spot size will be tuned to fill the aperture of the final focus lens. If the laser M^2 is then increased, the laser beam would clip the aperture and so the input beam will need to be re-tuned to reduce the size of the beam incicent on the lens by a factor M; this will consequently further increase by a factor M the spot size at the waist downstream of the lens. As a result the spot-size at the waist will have increased by a factor of M^2, as shown in Fig. 6.

In the following, the conventions used define y along vertical and x along the laser-beam direction. Including all the effects of M^2 and practicalities of light transport, the relevant formulae for Gaussian beam propogation are then modified as follows.

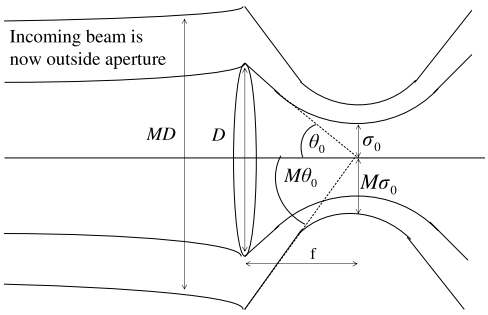

Figure 5: *Effect of $M^2 > 1$ on a LW final focus system initially set up to be optimised for $M^2 = 1$. In the unconstrained case, both the local angular divergence of the beam and its transverse spot dimension are increased by a factor of M.*

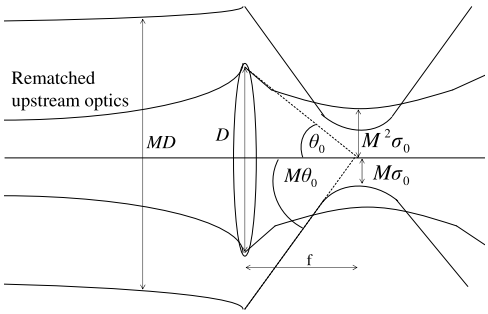

Figure 6: *Effect of rematching upstream optics for a beam with $M^2 > 1$ so as to maintain an optimised use of the final focus aperture. The final divergence of the lens must be reduced, by retuning the upstream laser optics, such that the beam is contained within the final focus aperture. This means that the transverse spot size at the waist must be further increased by a factor of M. Thus overal, the laser spot size at the waist is $M^2\sigma_0$.*

The light intensity of the laser has the form

$$I_\ell(x,y,z) = \frac{I_0}{2\pi\sigma_\ell^2}\frac{1}{f_R(x)}\exp\left[-\frac{y^2+z^2}{2\sigma_\ell^2 f_R(x)}\right] \qquad (26)$$

$$f_R(x) = 1 + \left(\frac{x}{x_R}\right)^2 \qquad (27)$$

$$\sigma_\ell = M^2 k_p \sigma_0 \qquad (28)$$

where $\sigma_0 = 0.5\lambda f_\#$ and, conservatively, $k_p \simeq 2$.

$$x_R = M^2\frac{4\pi\sigma_0^2}{\lambda} \qquad (29)$$

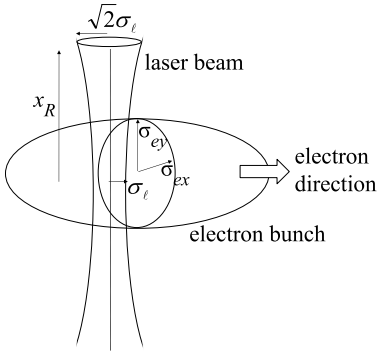

Figure 7: *Principle of operation of the laser-wire scanner with the key dimensions labeled. The figure shows the laser configured to scan the horizontal x-profile of the electron bunch σ_{ex}. x_R is the "Rayleigh range" of the laser beam as defined in Eq. 29; it gives the distance between the focus and the point where the laser spot-size has diverged to $\sqrt{2}$ of its minimum value.*

LASER-WIRE

Traditionally the transverse dimensions of an electron beam have been measured by scanning a tungsten or carbon wire across the beam and measuring the resulting backgrounds as a function of relative position of the wire. This method has the disadvantage of being highly disruptive to the electron beam and so it cannot be used during normal luminosity running. At the ILC, the electron beams in the BDS will have vertical transverse size of order 1-few μm; a normal wire scanner would not be able to measure beams of this size, nor would it be able to withstand the energy depositions from such high intensities. To solve these issues, the solid wire can be replaced by a finely-focused beam of laser light; such a system is called a laser-wire (LW).

Principle of Operation

The Compton collisions between laser photons and beam electrons are detected downstream and the Compton rate as a function of relative positions of electron and laser beams provides the measurement of the electron beam transverse profile. This principle is illustrated in Fig. 7, with a schematic experimental arrangement shown in Fig. 8. Two distinct methods have been employed to date. Operating the laser in continuous wave mode together with an optical cavity to enhance the power has been used [8] at the ATF at the KEK laboratory to measure the emittance of the damping ring; this technique would also be applicable to the ILC damping rings. In other parts of the machine, including the BDS, the beam is not circulating so a single-pass method based on high power pulsed lasers is required [9, 10, 11].

The Compton cross section decreases as the electron beam energy increases. For an electron beam energy E_b and laser photon energy $k = \frac{hc}{\lambda}$, the Compton cross sec-

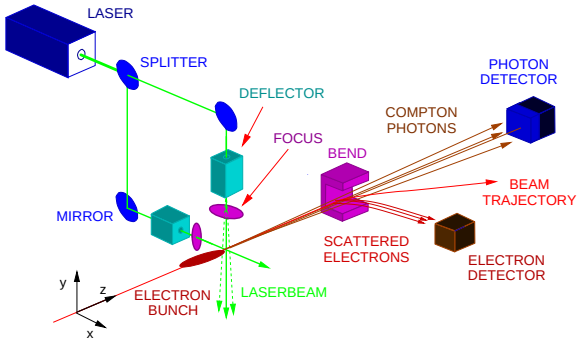

Figure 8: *Schematic of a practical LW system.*

Table 3: *Values of $f(\omega)$ for various laser wavelengths λ and ILC beam energies*

	λ(nm)			
E_b(GeV)	1064	532	355	266
5	0.96	0.92	0.89	0.86
50	0.72	0.59	0.51	0.45
150	0.51	0.38	0.31	0.27
250	0.41	0.30	0.24	0.20
500	0.30	0.20	0.16	0.13

tion is given by $\sigma_C(\omega) = \sigma_T f(\omega)$ where σ_T is the Thomson cross section = 0.665×10^{-28}m^2, $\omega = \frac{kE_b}{m_e^2}$, and $f(\omega)$ gives the ratio of Compton to the Thomson cross section. Values of $f(\omega)$ for laser wavelengths and beam energies of typical interest at the ILC [1] are presented in Table 3.

In this section, the Compton rate for a set of laser-wire operating conditions is derived as a function of relative horizontal and vertical offsets, Δ_x and Δ_y respectively, between the centroids of the electron bunch and laser beam.

The number $N(\Delta_x, \Delta_y)$ of Compton photons produced will be proportional to the relevant overlap integral, $\epsilon(\Delta_x, \Delta_y)$. In Sec. , $\epsilon(\Delta_x, \Delta_y)$ will be evaluated in μm^{-1}.

$$N(\Delta_x, \Delta_y) = N_0 \epsilon(\Delta_x, \Delta_y)$$

where

$$N_0 = \frac{P_\ell N_e \lambda f(\omega) \sigma_T}{hc^2} , \qquad (30)$$

P_ℓ is the instantaneous laser power at the laser-electron IP, and N_e is the number of electrons in the bunch. If $\eta_{\rm det}$ is the detector efficiency then, using realistic numerical values, the number of detected photons is $N_{\rm det}\epsilon(\Delta_x, \Delta_y)$, where

$$N_{\rm det} = 1212 \times \xi \qquad (31)$$

and

$$\xi = \frac{\eta_{\rm det}}{0.05} \frac{P_\ell}{10\ {\rm MW}} \frac{N_e}{2 \times 10^{10}} \frac{\lambda}{532\ {\rm nm}} \frac{f(\omega)}{0.2}\ \mu{\rm m} . \qquad (32)$$

Laser-Wire Overlap Integral

In the following, the electron beam is assumed to have a simple Gaussian charge profile, with σ_{ex} and σ_{ey} being the horizontal and vertical electron spot-sizes respectively. σ_z is assumed long compared to the laser spot-size, so the overlap integral in z integrates out trivially.

Scans Using the Laser TM$_{00}$ Mode

The full overlap integral of a TM$_{00}$ laser mode with a Gaussian electron bunch is now presented, including full effects of Rayleigh range. For the laser TM$_{00}$ mode, performing the z- and y-integrals gives [1]

$$\frac{I_\ell I_e}{2\pi\sigma_{ex}} \int_{-\infty}^{\infty} \frac{dx}{\sigma_s(x,\Delta_x)} \exp\left[-\frac{x^2}{2\sigma_{ex}^2} - \frac{\Delta_y^2}{2\sigma_s(x,\Delta_x)^2}\right] \qquad (33)$$

where

$$\sigma_s(x,\Delta_x) = \sqrt{\sigma_{ey}^2 + \sigma_\ell^2 f_R(x-\Delta_x)} . \qquad (34)$$

In the approximation of an infinite Rayleigh range the equations reduce to the more familiar form with [4]

$$\sigma_m = \sqrt{\sigma_e^2 + \sigma_\ell^2} \qquad (35)$$

and

$$\epsilon(\Delta_y) = \frac{1}{\sqrt{2\pi}\sigma_m} \exp -\frac{(\Delta_y)^2}{2\sigma_m^2} . \qquad (36)$$

Similar additional formulae are provided in Ref [1] for laser-wire scans using the TM$_{01}$ mode.

Results for the case of laser-M^2=1.3 and f_1 final focus optics are shown in Fig. 9 for an electron bunch transverse Gaussian profiles with (a) $\sigma_{ey} = 1\ \mu$m, $\sigma_{\rm ex} = 10\ \mu$m and (b) $\sigma_{ey} = 1\ \mu$m, $\sigma_{\rm ex} = 100\ \mu$m; the effect of the Rayleigh-range is very apparent for the larger aspect-ratio.

Some recent experimental results obtained from the LW at the ATF extraction line are shown in Fig. 10, including a fit to function of the form of Eq 33. The detailed parameter extraction at the ATF is currently being analysed, however it is clear that the shape of the data is not pure Gaussian, and that the fit including Rayleigh range effects describes the data well.

Contributions to the Errors of a Laser-wire Measurement

A laser-wire scan will yield a measurement of the rate of Compton events as a function of position of the laser beam; this transverse scan size, σ_m, will be a convolution of machine related-effects and laser-related ones. The machine-related effects include bunch-to-bunch position jitter and residual dispersion at the laser-wire interaction point (IP) and are discussed in detail in Ref. [1]. The laser-related effects include laser pointing jitter, intensity (normalisation)

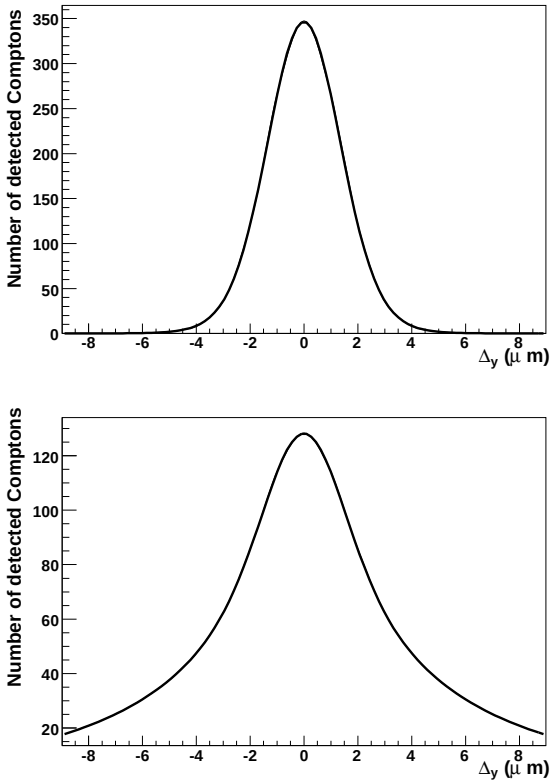

Figure 9: *Scan profile at the laser-wire IP for a laser with M^2=1.3 and wavelength 532* nm *operating in the TM_{00} mode and focused using f_1 optics. The electron bunch is assumed to have a Gaussian transverse profile. (a): $\sigma_{ey} = 1\ \mu\mathrm{m},\ \sigma_{\mathrm{ex}} = 10\ \mu\mathrm{m}$. (b): $\sigma_{ey} = 1\ \mu\mathrm{m},\ \sigma_{\mathrm{ex}} = 100\ \mu\mathrm{m}$*

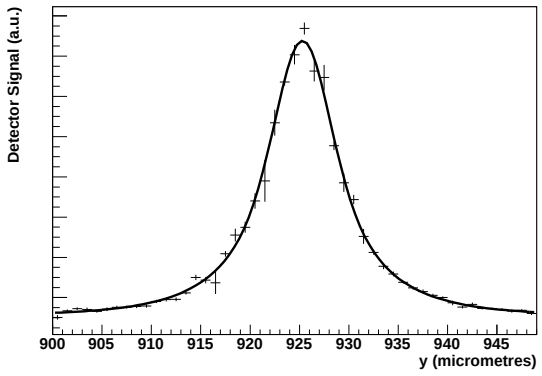

Figure 10: *Example scan from a laser-wire scan at the ATF extraction line. The non-Gaussian tails are clearly visible, which are well fit by including Rayleigh range effects, as given by Eq. 33*

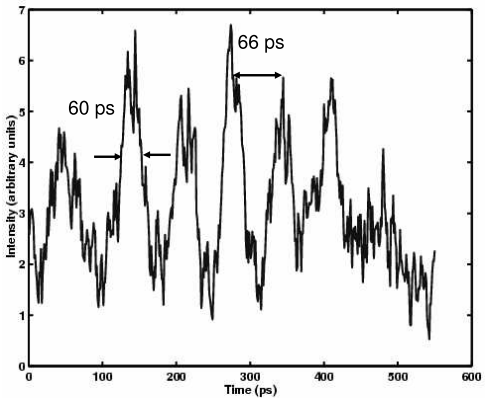

Figure 11: *Streak camera shot of a Q-switched laser. The temporal structure is due to longitudinal mode beating which, if the electron bunch lengths are less than or of order 50 ps, will have a serious impact on the effective rate at which a LW scan can be performed.*

fluctuations, and systematic errors associated with the uncertainty in the measurment of the light distribution at the IP, as discussed below.

Laser intensity fluctuations can be measured shot-by-shot using a fast photodiode; this works well for mode-locked systems, or for injection-seeded Q-switched ones. However, care must be taken with using unseeded Q-switched lasers because the presence of multiple longitudinal modes gives rise to a beating structure such as shown in Fig. 11, which is a streak-camera measurement of a Q-switched laser used in an early LW system at PETRAII. The PETRA bunch length is of order 50 ps, so shot by shot fluctuations of 100% are possible; this effect means that an average over several laser shots is required at each scan point. A later version of this system [10] used an injection seeded system, which enabled faster scan rates, as described below.

In the following a laser-wire scan is taken to consist of N_{scan} equally spaced values of y-displacements, Δ_y, of the laser with respect to the central value over a range $\pm 7\sigma_m$ (as defined in Eq. 35). The results presented here were obtained using $N_{\mathrm{scan}} = 19$, however the statistical errors can be scaled in the usual way for other values. The contributions to the raw laser-wire scan can be broken down as follows:

$$\left(\frac{\delta\sigma_{\mathrm{fit}}}{\sigma_{\mathrm{fit}}}\right)^2 = \frac{19}{N_{\mathrm{scan}}}\left(\frac{E_{\mathrm{stat}}}{\sqrt{\xi}} + E_\xi\right)^2 + E_{M^2}^2 \qquad (37)$$

where E_{stat} is the relative statistical error of a 19-point fit to the raw scan curve, ξ is the event rate normalisation as defined in Eq.32, and E_ξ is the relative error arising from the shot-by-shot normalisation fluctuations.

E_{M^2} is the relative error on the extraction of σ_e introduced by any uncertainty in the laser light distribution at

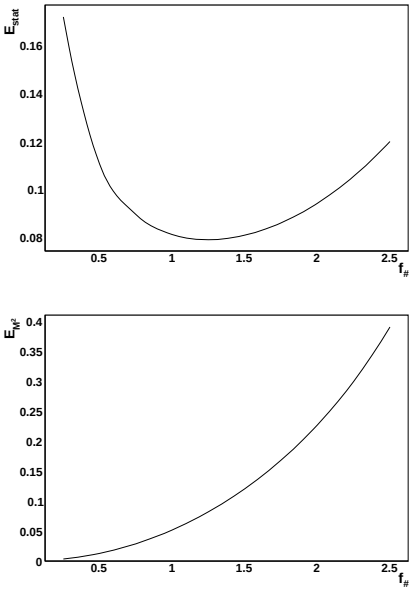

Figure 12: *(a): Statistical error $E_{\rm stat}$, (b): laser error E_{M^2} for $\xi = 1$ (Eq. 32) using $N_{\rm scan} = 19$ scan points versus the f-number of the final focus lens, using a laser with M^2=1.3 and operating in the TM$_{00}$ mode with $\lambda = 532\ nm$. The electron bunch is assumed to have a Gaussian transverse profile with $\sigma_{ey} = 1\ \mu$m and $\sigma_{ex} = 25\ \mu$m.*

the IP; this is characterized here by an error in the M^2 value of the laser and, for a real system, will need to be calculated including the effects of alignment errors etc. in the final-focus optics. Absolute M^2 measurements can be performed by slicing the laser-beam with a knife-edge at a set of longitudinal locations with respect to a laser-waist [17] and can be monitored relatively by capturing an image of the waist with a CCD camera.

E_{M^2} can be estimated by fitting the measured profile to σ_{ey} assuming a value of M^2 that is wrong by a factor $(1 + \delta_{M^2})$. In the following, the laser M^2 is thus assumed to be determined shot by shot to an accuracy of δ_{M^2}. Naively, without allowing for Rayleigh range effects, the error on the extracted value of σ_e from subtraction of the laser spot-size is

$$\frac{\delta\sigma_e}{\sigma_e} = \frac{\sigma_\ell}{\sigma_e^2}\delta\sigma_e \simeq \left(\frac{\lambda f_\#}{\sigma_e}\right)^2 M^2\delta_{M^2} \qquad (38)$$

Inserting representative values of $M^2 = 1.3$ and $\sigma_e = 1\ \mu$m gives:

$$\frac{\delta\sigma_e}{\sigma_e} = 1.08\left[\left(\frac{M^2}{1.3}\right)\left(\frac{1\ \mu\text{m}}{\sigma}\right)\left(\frac{\lambda}{532\ \text{nm}}\right)\left(\frac{f_\#}{1.5}\right)\right]^2\delta_{M^2}\ . \qquad (39)$$

A full numerical treatment [1] shows that this is a good approximation for small $\delta_{M^2} \simeq 1\%$ but is a slight underestimate for larger values.

The overlap integral Eq. 33 is now used to fit to a simulated laser-wire scan of interest to the ILC and thereby determine the laser-related errors on the extracted value of the electron vertical spot size σ_{ey}. Both $E_{\rm stat}$ and E_{M^2} will depend on the f-number of the laser optics employed. This dependence is illustrated in Fig. 12 for the case of $\sigma_{ey} = 1\ \mu$m and $\sigma_{ex} = 25\ \mu$m. For each set of σ_{ex}, σ_{ey}, there is an optimal f-number that gives the lowest statistical error for given values of ξ and $N_{\rm scan}$. However, as can be seen in Fig. 12, the minima are often fairly shallow, which must be contrasted with the difficulty of building low f-number optics. The difficulty is not just in building low f-number alone, but in producing a system that can maintain a small laser spot size approximately $\pm 10\ \sigma_\ell$ off axis, as needed during a scan. For these reasons, f-numbers of order 1.5 are likely to be optimal for ILC applications.

For larger spot-sizes and for the horizontal scans of the ILC electron bunch, the suitable f-number is determined primarily by the angular scan-range of the final focus lens plus scanning system. The laser optics for these dimensions will probably use diameter $D = 5$ cm optics (or similar). In this case, assuming again a scan range of $7\sigma_m$ the practical $f_\#$ is given by

$$f_\# = 1.4\left(\frac{\sigma_m}{10\ \mu\text{m}}\right)\left(\frac{5\ \text{cm}}{D}\right)\left(\frac{1\ \text{mrad}}{\theta_{\rm scan}^{\rm max}}\right)\ . \qquad (40)$$

In practice, for very large scan ranges, it may be preferable to use a stepping-motor system to move the final focus lens as opposed to scanning using optical ray deflection, which would enable smaller $f_\#$s to be employed. In that case, the scan would have to be very slow compared to the machine repetition rate. An additional consideration here is that the rate of Compton events is significantly lower for horizontal scans, due to the $1/\sigma_m$ factor in Eq. 36.

EXPERIMENTAL LW FACILITIES

Laser-wire at the PETRA Accelerator

A laser-wire system that can scan in both the horizontal and vertical directions was installed and operated [10] at the PETRAII accelerator. A schematic of this system is given in Fig. 13, which shows the stages used to find the beam and perform coarse scans using stepping motors. Faster, fine-grained, scanning was performed using mirrors attached to a piezo stack. Combined with the use of an inection-seeded Nd:YAG laser with wavelength λ=532 nm, high quality scans could be performed in about 50 s, this rate being limited by the repetition rate of the lase (20 Hz). Using both the horizontal and vertical scanning capability, the transverse beam profile was measured to be $46.5 \pm 0.6\ \mu$m in the vertical and $373 \pm 3\ \mu$m in the horizontal, where several single scans were used to obtain these measurements by fitting to the Rayleigh range formula of Eq. 29.

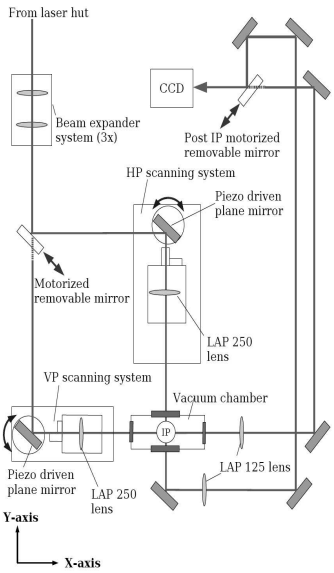

Figure 13: *Practical layout of a laser-wire system that can scan in both the horizontal and vertical dimensions. Such a system has operated at PETRAII [10]*

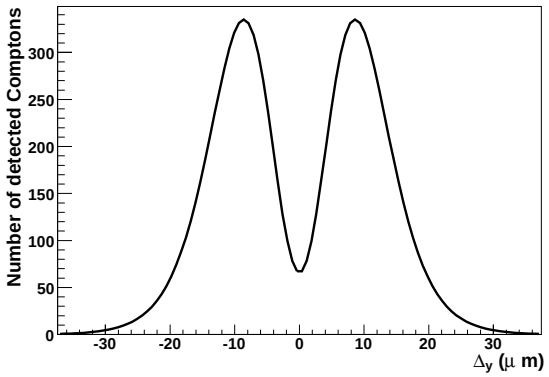

Figure 14: *Scan profile at the laser-wire IP for a laser with* M^2*=1.3 and wavelength 532* nm *operating in the* TM_{01} *mode and focused using* f_1 *optics. The electron bunch is assumed to have a Gaussian profile of* $\sigma_{ey} = 5\ \mu\mathrm{m},\ \sigma_{\mathrm{ex}} = 50\ \mu\mathrm{m}$

Laser-wire at H^- Accelerators

Laser-wires are also being used within H^- accelerators to measure the beam emittance [13]. They employ the photo dissociation technique, which is to ionize the H^- ions using lasers, which is possible because the threshold for this process is only about 0.75 eV and a Nd:YAG laser can thus be used as an effective light source. The laser light ionizes the H^- thus producing a free electron and a neutral H-atom. Both the electrons and the atoms can be used to determine detect the signal; the various components of the beam (H^0, H^- and e^-) are separated by a magnetic field and the electrons can then be detected in a Faraday cup to provide a fast signal that can also be used for a time-of-flight measurement in order to determine the longitudinal emittance of the electron bunch. The neutral atoms can be imaged by using a scintillation screen plus fast CCD camera [14]. The use of lasers in stripping the H^- ions to form an efficient source of protons is also being explored [15].

ALTERNATIVE MODES

Increased sensitivity to the electron spot-size can be obtained by using more sophisticated light distributions than the simple TM_{00} mode described above. Higher order laser-modes are one way to do this, another way is to create a laser interference pattern and scan the electron beam across the fringes; these methods are now discussed briefly.

TM_{01} laser mode

The case of operating the laser in TM_{01} mode with laser-M^2=1.3 and f_1 final focus optics are shown in Fig. 14 for an electron bunch transverse Gaussian profile with $\sigma_{ey} = 5\ \mu\mathrm{m},\ \sigma_{\mathrm{ex}} = 50\ \mu\mathrm{m}$; the benefit of the TM_{01} mode over similar scans using the TM_{00} mode (Fig. 9) is apparent due to the steeper variations of the signal as a function of Δ_y. The relative benefits of the TM_{00} and TM_{01} modes are discussed in Ref [1] , where it is shown that for $\sigma_{ey} > 1{-}2\ \mu$m there is a significant advantage for the statistical power by using the TM_{01} mode; this advantage has been demonstrated at the ATF [16]. However the sensitivity to the laser properties (as parameterized by a simple M^2 in these calculations) is greater for the TM_{01} mode and, for spot-sizes of order 1 μm, the relative statistical power of the TM_{01} to that of the TM_{00} mode decreases rapidly. The relative advantage of using higher order laser modes thus depends on where the system is located; laser-spot sizes of order 1 μm are of particular importance for the BDS LW system so the TM_{00} mode is more appropriate, whereas higher-order laser modes may be advantageous in other locations of the machine.

Interferometric Beam Size Monitor

The LW method of scanning across an electron bunch works well for electron bunch sizes greater than (or similar to) the wavelength of the light used (typically 0.5μm). For smaller electron bunches, an alternative technique has been demonstrated [4, 18], where a laser-beam is split into two and then the daughter beams superposed at a relative angle θ as shown in Fig 15. This sets up an interference pattern of the form [4]:

$$I(y) = I_0\left[1 + \cos\theta\cos\left(2k_y y\right)\right] \qquad (41)$$

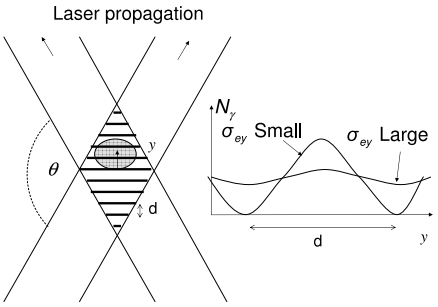

Figure 15: *Principle of an interferometric beam size monitor ("Shintake monitor"). The laser-beams are superposed at a relative total angle θ and the convolution of the resulting intensity fringes with a Gaussian electron bunch gives a number of Compton photons that varies as a function of relative position y between the fringes and the bunch. A measurement of the electron bunch size can be inferred from the magnitude of this signal variation, given by Eq. 42.*

where $k_y = 2\pi \sin(\theta/2)/\lambda$. This treatment applies only within that part of the region of overlap where a plane-wave approximation to Eq. 8 is valid (i.e. well within the Rayleigh range). If a Gaussian electron beam with rms size σ_{ey} is then incident on the region of overlap, the number of Compton photons N_γ is given by its convolution with Eq. 41:

$$N_\gamma = \frac{N_0}{2}\left(1 + \cos\left(2k_y y\right)\cos\theta \exp\left[-2(k_y\sigma_{ey})^2\right]\right) \tag{42}$$

This system, now frequently referred to as a "Shintake monitor", was employed [18] at the Final Focus Test Beam at SLAC, where the modulation of the Compton photon signal as a function of electron beam position determined the electron vertical spot size to be 73 nm. This system has since been transported to the ATF2 experiment [19] where it will be used to measure electron spot-sizes down to about 35 nm. In principle, through the use of shorter wavelength light, measurements of spot-sizes down to about 10 nm may eventually be possible using this technique, although this will require additional R&D both on the laser systems themselves and on the control of vibrations and jitter.

SUMMARY

Lasers are important elements of advanced beam diagnostics systems for transverse bunch profile measurements, with uses in both electron and proton machines. The main elements of such systems were described, including a derivation of the key formulae. A brief overview of exisiting laser-based systems was provided, with references to more detailed discussions in the literature.

REFERENCES

[1] I Agapov, G. A. Blair, M. Woodley. "Beam emittance measurement with laser wire scanners in the ILC beam delivery system". Phys. Rev. ST Accel. Beams **10**, 112801 (2007).

[2] Barish, B. and others. "ILC Reference Design Report" (2007). http://www.linearcollider.org/cms/

[3] Balakin, V. and others, "Focusing of submicron beams for TeV Scale e+ e- linear colliders". Phys. Rev. Lett. **74** 2479-2482 (1995).

[4] Tenenbaum, P. and Shintake, T., "Measurement of small electron-beam spots", Ann. Rev. Nucl. Part. Sci. **49** 125-162 (1999)

[5] Minty, M. and Zimmermann, F., "Measurement and Control of Charged Particle Beams" Springer (2003)

[6] Wiedemann, H., "Particle Accelerator Physics I",Springer (1999).

[7] Seeman, J., "Transverse and Longitudinal Emittance Measurements" in "Handbook of Accelerator Physics and Engineering", Ed. Chao, A. and Tigner, M., World Scientific, 559-562 (1999).

[8] Honda, Y. and others, "Upgraded laser wire beam profile monitor" Nucl. Instrum. Meth.,**A538** 100-115 (2005).

[9] Grishanov, B. I. and others, "ATF2 proposal. Vol. 2", physics/0606194 (2006)

[10] A. Bosco and others, "A Two Dimensional Laser-Wire Scanner for Electron Accelerators", to appear in NIM A (2008).

[11] Boogert, S. T. and others, "A laser-wire system at the ATF extraction line", Prepared for Particle Accelerator Conference (PAC07).

[12] Siegman, A. E.,"Lasers", University Science Books (1986).

[13] S. Assadi, "SNS Transverse and Longitudinal laser profile monitors desing, implementation and results", Proc. EPAC06 (2006).

[14] C. Gabor and others, "Laser-based Beam Diagnostic for the Front End Test Stand (FETS) at RAL", Proceedings of EPAC06 (2006).

[15] Danilov, V. and others, "Proof-of-principle demonstration of high efficiency laser-assisted H^- beam conversion to protons", Phys. Rev. ST Accel. Beams **10** 053501 (2007),

[16] Y. Honda, "Laser-wire at ATF Damping Ring", Proc. Laser-wire Mini Workshop, Oxford, (2006).

[17] T. F. Johnston, "Beam propagation (M^2) measruement made as easy as it gets: the four cuts method", Applied Optics **37**, 4840-4850 (1998).

[18] Balakin, V. and others, "Focusing of Submicron Beams for TeV-Scale e^+e^- Linear Colliders", Phys. Rev. Lett. **74** 2479-2482 (1995).

[19] Grishanov, B. I. and others, "ATF2 proposal. Vol. 2", physics/0606194 (2006).